White paper

Titanium Contrast-Enhanced Mammography (TiCEM)

Expand your diagnostic insights

Johannes G Korporaal, PhD, Mathias D Hörnig,
Thomas Mertelmeier, PhD and Axel Hebecker, PhD

SIEMENS Healthineers

Contents

1. Introduction **3**

2. Contrast-enhanced imaging **4**

2.1 Physiology 4

2.2 Contrast enhancement in healthy breast tissue 5

2.3 Contrast enhancement in tumors 5

2.4 Measuring contrast enhancement: dynamic or static 6

2.5 Safety 6

3. Dual-energy imaging **7**

3.1 Attenuation of X-rays 7

3.2 Why dual-energy imaging? 8

3.3 Choice of X-ray spectra 9

3.4 Image processing 10

4. TiCEM – Titanium Contrast-Enhanced Mammography **11**

4.1 Clinical workflow 11

4.2 Image acquisition 12

4.3 Image post-processing 13

5. Clinical performance **14**

5.1 Sensitivity and specificity 14

5.2 TiCEM studies and sample cases 15

6. Discussion & conclusions **19**

6.1 Clinical indications for TiCEM 19

6.2 Comparison with MRI 19

6.3 Combinations with other technologies 20

6.4 Conclusions 21

7. Abbreviations **22**

8. References **23**

Please note:

In this white paper, the term CEDEM refers to the methodology in general (also known as CESM). TiCEM refers to the product implementation of Siemens Healthineers.

1. Introduction

Full-field digital mammography (FFDM) is currently the gold standard when it comes to breast cancer screening [1]. It delivers high-resolution images of the breast in a short amount of time. However, there is one limitation inherent in this acquisition method: tissue superimposition. To help solve this issue, digital breast tomosynthesis (DBT) has been introduced in clinical practice in recent years. It provides 3D information on breast tissue by acquiring images at different angles and results in higher cancer detection rates [2–4]. DBT is becoming an established method in clinical routine, and may in the near future replace digital mammography as the breast screening imaging modality of choice.

Both FFDM and DBT are morphological techniques, showing tissue structures rather than physiology. Although this might be sufficient to detect abnormalities in a screening setting, for diagnostic workup of recalled women, additional functional imaging techniques might offer a significant diagnostic advantage by visualizing atypical physiological processes.

For X-ray mammography systems, contrast-enhanced dual-energy mammography (CEDEM) is the functional imaging technique that has shown the greatest potential in this respect. CEDEM is a combination of **contrast-enhanced (CE) imaging**, known from computed tomography (CT), angiography and magnetic resonance imaging (MRI), and **dual-energy (DE) imaging**, known from CT and dual-energy X-ray absorptiometry (DXA).

Siemens Healthineers has entered the CEDEM market with its unique TiCEM application as an option on the MAMMOMAT Revelation, featuring a dedicated titanium filter that offers key advantages. This white paper will:

- present the scientific background and opportunities for the CEDEM methodology;
- highlight the specific features of TiCEM and its clinical workflow;
- review the scientific literature for the most prominent achievements to date; and
- discuss clinical and technological challenges.

The first part of this white paper (Chapters 2 and 3) will have an educational character, with a strong focus on imaging principles. The second part will provide more technical and clinical details about TiCEM (Chapters 4 and 5), and the final part discusses its current status as well as future directions (Chapter 6).

2. Contrast-enhanced imaging

The use of contrast agents is common practice in radiology, for example in CT [5], MRI [6] and ultrasound (US) [7]. The purpose of injecting a contrast agent is to increase the visibility of vascular structures or to visualize contrast agent uptake in tissues. As contrast enhancement depends on the tissue type, pathological processes might show abnormalities in contrast agent uptake and enable detection of malignancies. And since mammography is based on the attenuation of X-rays, the choice of iodine-based contrast agents, which are also used in CT, is obvious.

2.1 Physiology

After an iodinated contrast agent has been intravenously injected, it will traverse the lungs and the heart (twice) before it enters the systemic circulation. From the aorta, the contrast agent is then distributed throughout the body to the organs and tissues. Although a large part of the contrast agent will stay within the arteries during its first pass through the body, over time the contrast agent will leak out of the capillaries into the extravascular extracellular space, also known as interstitial fluid. Depending on the blood flow, on the volume percent of extravascular extracellular space and on vessel permeability ("leakiness"), a certain amount of contrast agent will accumulate in a tissue and give rise to a signal enhancement during imaging (Figure 1). The entire process of how contrast agents behave inside the human body is called contrast agent kinetics, and can be described by means of tracer kinetic models [8, 9].

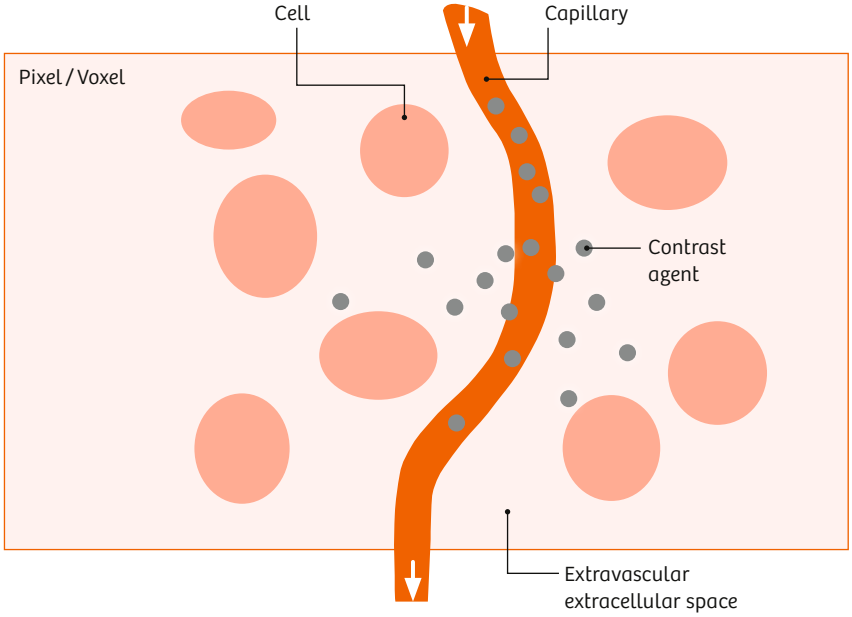

Figure 1: Depending on vessel permeability, blood flow and the amount of extravascular extracellular space, part of the contrast agent will accumulate in a tissue and give rise to a signal enhancement during imaging.

2.2 Contrast enhancement in healthy breast tissue

The human breast consists primarily of two different types of tissue: adipose and fibroglandular tissue. The contrast agent uptake in adipose tissue is typically very low, leading to almost no contrast enhancement over time [10]. Fibroglandular tissue, on the other hand, has a good vascular network and thus is well perfused. However, the blood vessels are not highly permeable, which results in a slow contrast agent uptake, a low amplitude and the contrast enhancement typically showing a plateau (Figure 2) [10].

This contrast agent uptake of healthy glandular tissue has been described in scientific literature as background parenchymal enhancement (BPE) and is a well-known phenomenon in MR imaging [11]. It is usually present in a bilateral, symmetrical distribution [11], with asymmetrical BPE being seen due to benign and malignant causes [12]. BPE is known to fluctuate with breast density, hormone levels (e.g. phase of the menstrual cycle, menopause, hormone therapy) and radiation therapy [11, 12], and has been demonstrated to be an independent predictor of breast cancer risk [11]. The amount of BPE is subjectively described as minimal, mild, moderate or marked enhancement [11–14] and can lead to decreased visibility of enhancing lesions, as these stand out less clearly from the background at higher BPE levels.

2.3 Contrast enhancement in tumors

For most invasive tumors, the formation of new blood vessels, called angiogenesis, is one of the pathophysiological processes characteristic of tumor growth [15]. Tumor cells initiate the formation of new vasculature from pre-existing vessels, often resulting in an irregular bed of leaky vessels. These abnormalities in tissue perfusion and contrast agent leakage lead to increased visibility of tumors in contrast-enhanced scans. The reason for this is that a lot of contrast agent is taken up by the tumor tissue due to the good blood supply. Furthermore, the leaky vessels allow the contrast agent to move into and out of the tumor tissue rapidly, a process commonly referred to in MRI literature as wash-in and wash-out [10]. Typical contrast-enhancement curves observed in the human breast are shown in Figure 2.

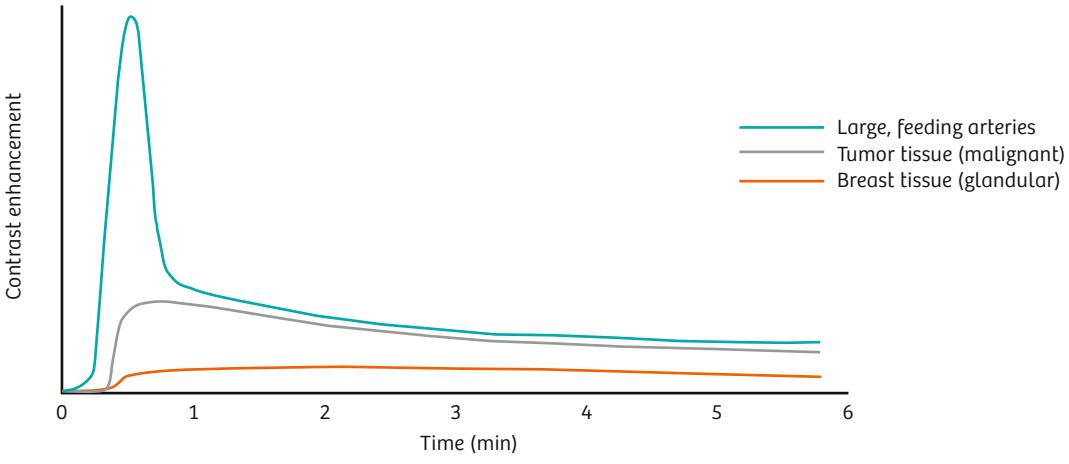

Figure 2: Differences in physiology, predominantly blood flow and vessel permeability, are reflected in the shapes and amplitudes of enhancement curves. Over time, all tissues will reach stable plateau phases, with tumor tissue generally having a higher enhancement level than healthy breast tissue (BPE) [10]. Please note: The purpose of this figure is to illustrate different enhancement patterns in general. The curves shown are estimated based on tracer kinetic models and are not actually measured inside a female breast.

2.4 Measuring contrast enhancement: dynamic or static

It would be desirable to perform repeated measurements over time to obtain information about the contrast agent dynamics and to capture the arterial phase of tumor enhancement characterized by a steep upslope and a rapid wash-out. This approach has been tested by subtracting a baseline image prior to injection from the subsequent images, as it is known from angiography procedures, for example. However, in clinical studies this so-called temporal subtraction mammography [16] has not been able to consistently demonstrate distinctly different patterns for benign and malignant lesions [17]. Furthermore, the most prominent factors hindering a successful implementation of this dynamic acquisition method are the high cumulative radiation dose of repeated acquisitions, the necessity for repeated contrast agent injections for each view and breast, as well as the breast compression that hinders normal blood flow into the breast [16–20].

This has two important implications for the implementation and workflow of CEDEM. First, the compression-induced restriction of blood flow into the breast means that patient positioning, breast compression and image acquisition should take place after the injection has been completed.

As a result, imaging the arterial phase of contrast enhancement is not possible. However, the contrast enhancement is more stable after the arterial peak (Figure 2), allowing for a larger timing window to perform the measurements. Also, differences in contrast agent uptake between malignant lesions and healthy tissue still permit differentiation of malignancies.

Second, differences in contrast agent uptake should be derived from independent measurements at single time points, as no baseline image (acquired prior to the injection) will be available. And since the iodinated contrast agent is not visible in a routine mammogram [21], there is a need for a different approach to extract the iodine signal at a single time point. This is where the dual-energy methodology comes into play, as will be explained in the next chapter.

2.5 Safety

As with all intravenous contrast agent injections, allergic reactions may occur, but can almost entirely be prevented by following regular safety guidelines for iodinated contrast agents [22, 23] as well as local standard operating procedures.

3. Dual-energy imaging

In FFDM, images are generated by measuring the attenuation of X-rays that have passed through the breast. Because of the working principle of X-ray tubes, the photons in the X-ray beam do not all have the same energy; they have different energies, resulting in an X-ray spectrum (Figure 3). The shape of an X-ray spectrum depends on:

- the peak voltage of the X-ray tube (kV);
- the anode material; and
- the filtering of the X-ray beam.

The peak voltage determines the highest photon energy in the X-ray spectrum, whereas the anode material influences the distribution of energies present in the spectrum. It is important to filter the X-ray beam before it reaches the patient, to reduce the number of low-energy photons. These would merely lead to higher radiation doses but would not contribute to the image. With additional filtering, specific photon energies can be filtered out of the beam, to increase or decrease the average energy of the X-ray spectrum (see paragraph 3.3).

3.1 Attenuation of X-rays

In X-ray based imaging modalities, the contrasts in the final image originate from differences in X-ray absorption inside a scanned object. X-ray absorption in turn depends on both the physical density and chemical composition of the object. The effect of chemical composition on X-ray absorption can be described by means of the mass attenuation coefficient, which is material-specific and depends on the photon energy. This energy dependence is illustrated in Figure 4, which shows the mass attenuation coefficients for several types of tissue as a function of photon energy [24]. The higher the mass attenuation coefficient of a material is, the more photons are absorbed. Since breast tissue is a mixture of adipose and soft tissue (glandular or tumor tissue), the curve for breast tissue (black line in Figure 4) lies between the curves for adipose and soft tissue.

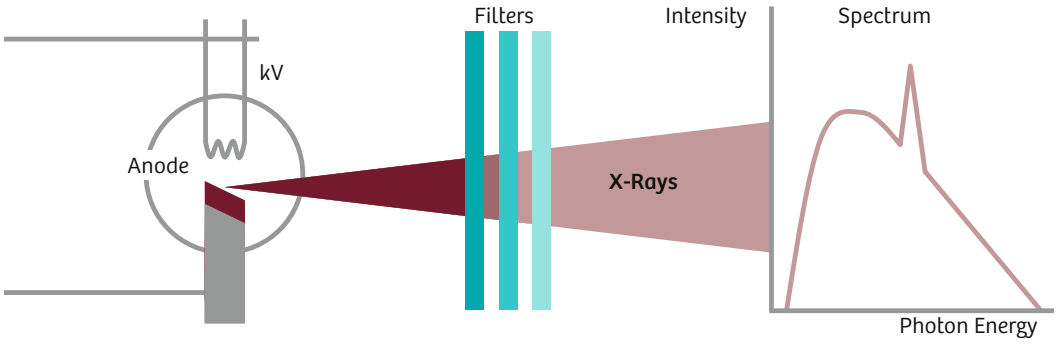

Figure 3: The shape of an X-ray spectrum depends on the peak voltage of the X-ray tube (kV), the anode material and the filtering of the X-ray beam.

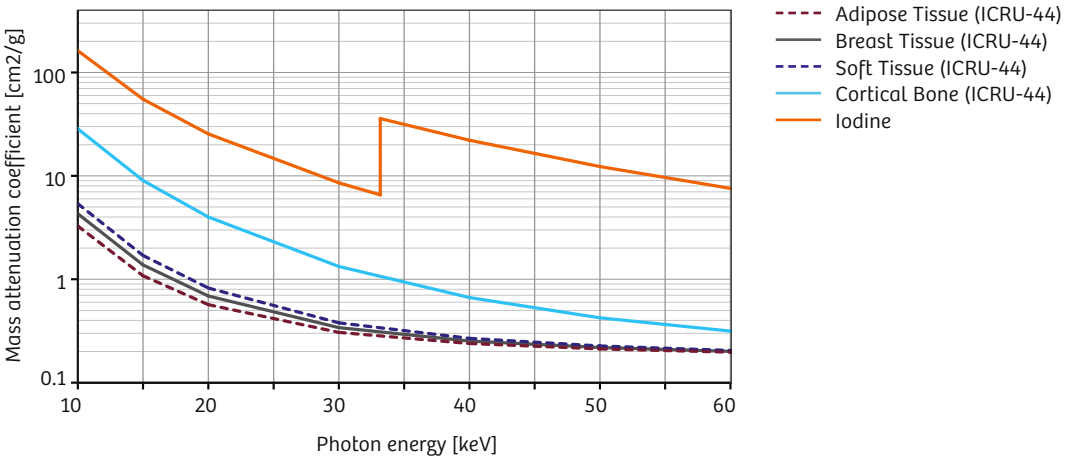

Figure 4: Mass attenuation coefficients for several types of tissue [24]. The higher the mass attenuation coefficient of a material is, the more photons are absorbed. The K-edge of the iodine atom leads to a sudden increase in the mass attenuation coefficient at 33.2 keV.

3.2 Why dual-energy imaging?

Whereas standard mammography is performed using one X-ray spectrum ("single-energy"), the term "dual-energy" refers to imaging a tissue using two different spectra. Its advantage is that two materials can be discriminated if the difference in their mass attenuation coefficient is significantly different for the two X-ray spectra.

Since both tumor tissue and healthy fibroglandular tissue are soft tissues, they have the same mass attenuation coefficient for all energies (dashed blue line in Figure 4) and cannot immediately be differentiated by means of dual-energy imaging. However, as explained in Chapter 2, differences in iodine uptake between healthy glandular and tumor tissue exist. And as the mass attenuation coefficient between soft tissue and iodine is significantly different (Figure 4), an iodine map can be calculated, showing contrast agent uptake, being indicative for tumor tissue.

Especially in dense breasts, where the iodine contrast might be hidden under or confused with high-intensity fibroglandular tissue in a normal, single-energy mammogram, dual-energy acquisitions can have a definite advantage, as illustrated in Figure 5.

Despite the much higher mass attenuation coefficient of iodine compared to soft tissue, the iodinated contrast agent cannot be seen in normal FFDM images (single-energy), although present in the tissue [21]. This is due to its very low concentration, resulting in only very slightly increased pixel intensities.

Therefore, contrast-enhanced dual-energy mammography is a result of:

- differences in the mass attenuation coefficient between breast tissue and iodine; and
- differences in contrast agent uptake between tumor and fibroglandular tissue.

3.3 Choice of X-ray spectra

When performing dual-energy mammography, two different X-ray spectra must be selected. Finding a good combination of X-ray spectra is a complex task and will unquestionably involve a trade-off, since many factors need to be taken into account.

The mass attenuation coefficient of iodine shows a characteristic step at 33.2 keV, the so-called K-edge (Figure 4). This is an important peak, since for photon energies just below 33.2 keV, the attenuation will be much lower compared to photon energies just above this K-edge. Since the attenuation of breast tissue is almost the same either side of 33.2 keV, a difference in iodine contrast in the mammogram can be expected for X-ray spectra just below and just above 33.2 keV. So from a physics point of view, two narrow spectra, one just before and one just after the K-edge of iodine, would be optimal.

For the low-energy spectrum, filter materials with K-edges just below 33.2 keV are of interest, because almost all photons with energies higher than that K-edge will be absorbed. This results in an abrupt, very well defined end of the spectrum and allows for precise shaping of the X-ray spectrum.

For the high-energy spectrum, the use of additional filtering with high-Z (high atomic number) materials is also beneficial. By increasing the filter thickness, the average beam energy can be increased and the spectrum will become narrower. However, a thicker filter will also absorb more X-rays and therefore necessitates a higher tube output to obtain the same radiation dose in the tissue. So, the maximum filter thickness is always dependent on the maximum output of the X-ray tube and should be tailored to its heat capacity.

Together with other practical constraints, such as the maximum available space in the filter box, the availability of the filter material and the processing options and costs, the selection of a good combination of X-ray spectra is challenging and trade-offs are unavoidable.

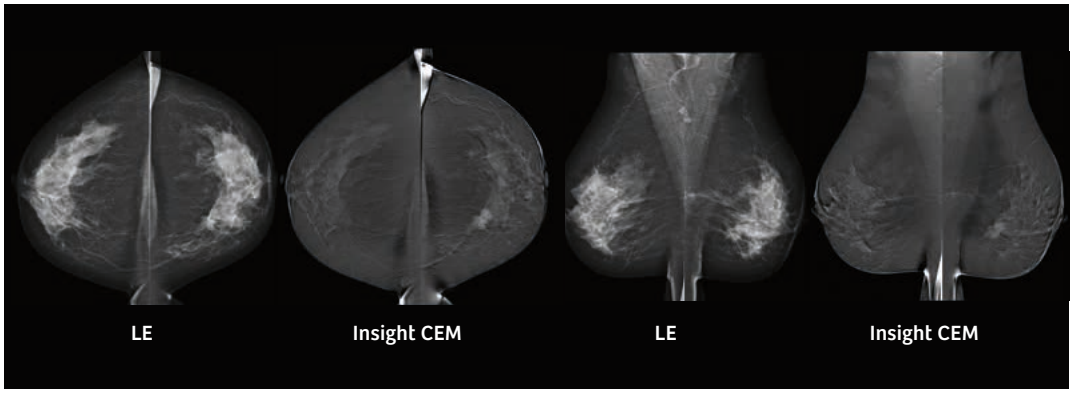

Figure 5: Clinical example of a 52-year-old female presenting a palpable tumor in her left breast (two foci, invasive ductal carcinoma (IDC) grade 1 with parts of ductal carcinoma in situ (DCIS)). The low-energy (LE) images show dense fibroglandular tissue, without clear lesions taking up contrast agent. In the recombined Insight CEM image, the anatomical background is neutralized by the weighted subtraction and the lesion becomes clearly visible. (Images courtesy of Dr. I. Vejborg, Copenhagen, Denmark)

3.4 Image processing

As CEDEM is implemented on a standard mammography system, the high-energy (HE) and low-energy (LE) images must be acquired successively, resulting in a time difference between the two acquisitions. For this reason, image acquisition is performed during the venous phase, where the changes in contrast enhancement over time are only minor. Because of the time difference between the successive acquisitions, patient motion may occur even though the breast is compressed. In such cases, image registration could be of help before further processing of the LE and HE images.

When high- and low-energy mammograms are in alignment, a particular material, for example soft tissue or iodine, can be highlighted by removing the other materials from the image. This can be done using a weighted subtraction. By adjusting the weighting factor to a certain material, the contrast difference produced in that material by the two different X-ray spectra can be neutralized, resulting in suppression of the material in the final image. In the case of contrast-enhanced dual-energy mammography, the image contrasts for fibroglandular tissue will be removed from the image, resulting in an increased image contrast of the iodine uptake inside the breast (Figure 6).

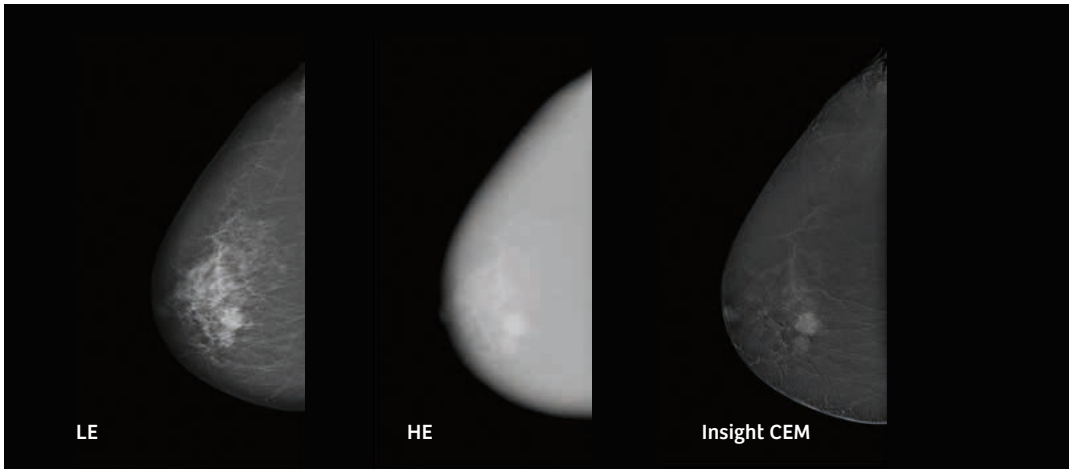

Figure 6: Clinical example of a 65-year-old female who underwent a TiCEM examination. The low-energy (LE) image shows at least one suspicious hyperdense area inside the fibroglandular tissue. After the weighted subtraction of the high-energy (HE) image (see Chapter 4.3), the recombined Insight CEM image reveals the contrast agent uptake without masking of the fibroglandular tissue. Histological analysis confirmed an invasive ductal carcinoma (IDC) grade 2 as well as a high-grade ductal carcinoma in situ (DCIS) with comedo necrosis and calcifications. (Images courtesy of Prof. Dr. D. Uhlenbrock, Dortmund, Germany)

4. TiCEM – Titanium Contrast-Enhanced Mammography

With the introduction of the MAMMOMAT Revelation, Siemens Healthineers has implemented its CEDEM application as Titanium Contrast-Enhanced Mammography (TiCEM). TiCEM aims at improving diagnostic accuracy in the detection and characterization of breast tumors, by incorporating functional information.

4.1 Clinical workflow

The clinical workflow for a TiCEM examination (Figure 7) starts with the injection of the iodinated contrast agent by means of a power injector. At the time of injection, the breast is not (yet) compressed, to allow for normal tissue perfusion and unhindered inflow of the contrast agent into the breast. The dosage of the contrast agent is typically weight-dependent and varies between institutions (Table 1).

Study	Dosage [mL/kg]	Iodine concentration [mg/mL]	Flow [mL/s]	Scan delay [min]	Power injector
[25]	1.5	300	3	2	Yes
[26]	1.5	300	3	2	Yes
[27]	1.5	300	3	2	Yes
[28]	1.5	300/350	3	2.5–5	Yes
[29]	1.5	350	3	2	Yes
[30]	1.5	350	3	2	Yes
[31]	1.5	350	3	2	Yes
[11]	1.5	350	3	2.5	Yes
[32]	1.5 (max 90mL)	350	3	2	Yes
[33]	90mL for all	350	3	2	Yes
[34]	1.5	370	3	2	Yes
[35]	1.5	370	3	2	Yes
[36]	2.0	400	3.5	1–1.5	Yes

Table 1: Injection protocol parameters from scientific literature. Note that in these studies the iodine dose (dosage x concentration) ranges from 0.45 to 0.80 gI/kg (grams of iodine per kilogram body weight), which is almost a two-fold difference.

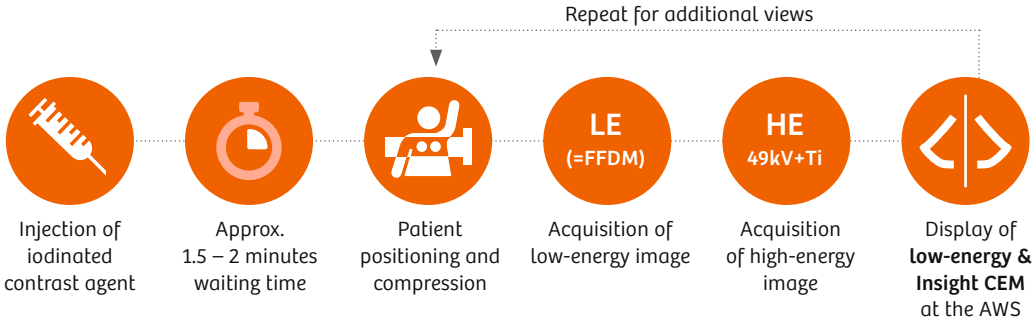

Figure 7: Simplified workflow illustration. The workflow may vary depending on the method used, patient situation and individual preferences.

After a waiting time of approximately 2 minutes (see Table 1), the woman is positioned at the MAMMOMAT Revelation and the breast is compressed. Then, a low-energy (LE) and a high-energy (HE) image are acquired successively and an Insight CEM image, a recombined image of that view (see 3.4), is calculated. These steps are then repeated for each additional view, without the need to perform a new contrast agent injection.

The time window for performing multiple views with a single contrast agent injection lasts up to 10 minutes [28], although the views should be acquired without any unnecessary delays. The order in which the views are acquired seems to be of little clinical significance [28] and does not appear to affect image quality [30].

Care should be taken when handling the contrast agent to avoid contamination of the detector or the skin with pure contrast agent, as this might mimic calcifications or result in artifacts [37, 38].

4.2 Image acquisition

The LE image is acquired first, all acquisition parameters being identical to those of a normal FFDM acquisition with a tungsten (W) anode target with a 50µm rhodium (Rh) filter and a tube voltage between 28 and 32kV. As previously explained (Chapter 3), the contrast agent uptake, although present in the tissue, is practically invisible in this LE image [21].

Subsequently, the HE image is acquired at 49kV with the unique titanium filter, which substantially reduces the X-ray tube load and enables uninterrupted acquisitions. Compared to other potential filter candidates such as a 0.3mm copper filter, the 1mm titanium filter allows for a 60% higher tube output at equal image quality (Figure 8) [39]. This results in a lower risk of tube overheating and means that, even for thick and dense breasts requiring a higher average glandular dose (AGD), sufficient tube power is available to obtain adequate image quality.

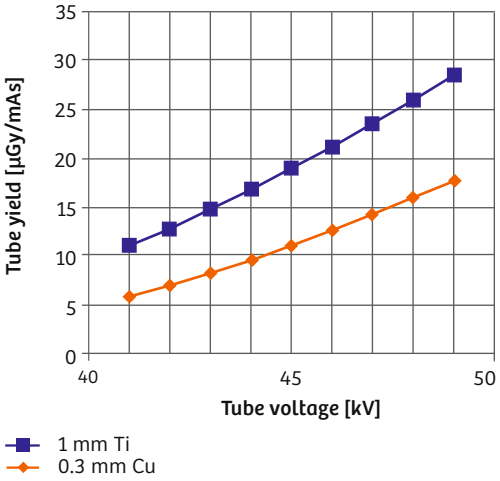

Figure 8: Simulated tube outputs in µGy/mAs of a tungsten anode target with a 1.0 mm titanium and 0.3mm copper filter (650mm from focal spot) [39]. The 1mm titanium filter allows for a 60% higher tube output at equal image quality.

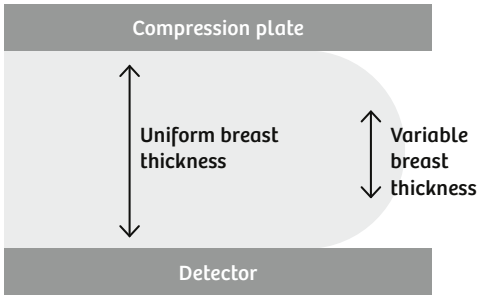

Figure 9: The TiCEM image post-processing suppresses artifacts at the borders of the breast, where the compressed breast thickness is not uniform.

The radiation dose (AGD) of the LE acquisition equals that of a normal FFDM acquisition, whereas the additional dose of the HE acquisition can reach a maximum of ~50% of the normal AGD of an FFDM image. As TiCEM examinations will be performed only in the context of diagnostic work-up and not screening, this increase in radiation dose can be justified in view of the increased diagnostic power to detect or rule out lesions.

4.3 Image post-processing

To obtain the recombined image, called Insight CEM, image processing of the LE and HE images is required. A weighted subtraction of the logarithmic high-energy (HE) and low-energy (LE) images is performed:

$$\ln(\text{Insight CEM}) = \ln(\text{HE}) - w * \ln(\text{LE}) \qquad \text{[eq. 1]},$$

where ln is the natural logarithm and w the weighting factor [36]. The TiCEM image post-processing suppresses artifacts at the borders of the breast, where the compressed breast thickness is no longer constant (Figure 9) [34, 36].

5. Clinical performance

In contrast to FFDM, there are no standardized interpretation criteria for the evaluation of breast lesions in CEDEM. Nonetheless, in scientific literature the application of BI-RADS descriptors for MRI has been shown to be useful for describing enhancement in recombined images [13]. Contrast enhancement is often classified according to a four-point scale, e.g. none, mild, moderate or marked, and mass and non-mass enhancement are described separately [12, 36, 40].

Reading of TiCEM examinations is generally performed by looking at the paired LE and Insight CEM images, without incorporating the HE image. As the Insight CEM image primarily shows iodine uptake and not morphological structures, the LE image can be used for navigating lesions inside the breast. The reading solution *syngo*.Breast Care offers dedicated layouts for TiCEM examinations and enables toggling between the LE and Insight CEM images.

enhancement can also be found in benign breast lesions [41]. Interestingly, a detailed description of, and systematic correlation between the particular enhancement behaviors and the different lesion types is lacking, whereas most cases with false positive and false negative findings have been extensively described, e.g. [26, 28, 32, 40, 42–45, 33, 46].

When it comes to diagnostic accuracy, sensitivity and specificity have been measured in several studies and summarized in a systematic review by Tagliafico et al [47]. They found a very high overall sensitivity of 98%, a very low specificity of 58% and an area under the ROC curve of 0.93 [47]. These numbers should, however, be interpreted with caution, as most studies are based on highly selected case series and prone to selection bias. This means that the study cohorts had a very high prevalence of breast cancer (up to 100% [26]), thereby prejudicing these diagnostic measures of CEDEM.

5.1 Sensitivity and specificity

Several studies have investigated the sensitivity and specificity of the CEDEM methodology. For such an analysis, positive and negative findings need to be defined and thus malignant and benign findings described (see Table 2).

Reports in scientific literature have shown contrast enhancement in almost all malignant lesions of the breast, although contrast

Malignant	Benign	
Invasive ductal carcinoma	Fibroadenoma	Intramammary lymph node
Invasive lobular carcinoma	Simple cyst	Sclerosing adenosis
Ductal carcinoma in situ	Reactive changes / benign	Atypical lobular hyperplasia
Invasive mucinous carcinoma	Apocrine changes / metaplasia	Ductectasia
Invasive micropapillary carcinoma	Papilloma	Fibrosis
	Superposition	Ductal hyperplasia
	Cylindrical cell changes	Lobular carcinoma in situ
	Old hematoma	Flat epithelial atypia
	Inflammation	

Table 2: Several malignant and benign lesions and subtypes of invasive cancers have been reported in scientific literature [26].

5.2 TiCEM studies and sample cases

In a clinical feasibility study, Knogler et al. used the TiCEM prototype in 15 patients with suspicious findings from FFDM (ACR BI-RADS 4 & 5) [36]. Imaging was performed 60-90 seconds after administration of the contrast agent. For the interpretation of the Insight CEM images, the criteria from the MRI part of the BI-RADS lexicon were used. TiCEM revealed more lesions than FFDM alone, and all malignant lesions showed a strong contrast enhancement. Benign lesions showed moderate or no enhancement.

After adding Insight CEM images to the FFDM findings, the BI-RADS assessment changed in 10 out of 15 patients (66.7%). This demonstrated the feasibility and additional value of the TiCEM prototype in a clinical setting (Figure 10) [36].

The following clinical cases (Figures 10–13) were gathered from the clinical use tests performed prior to the market introduction of the MAMMOMAT Revelation.

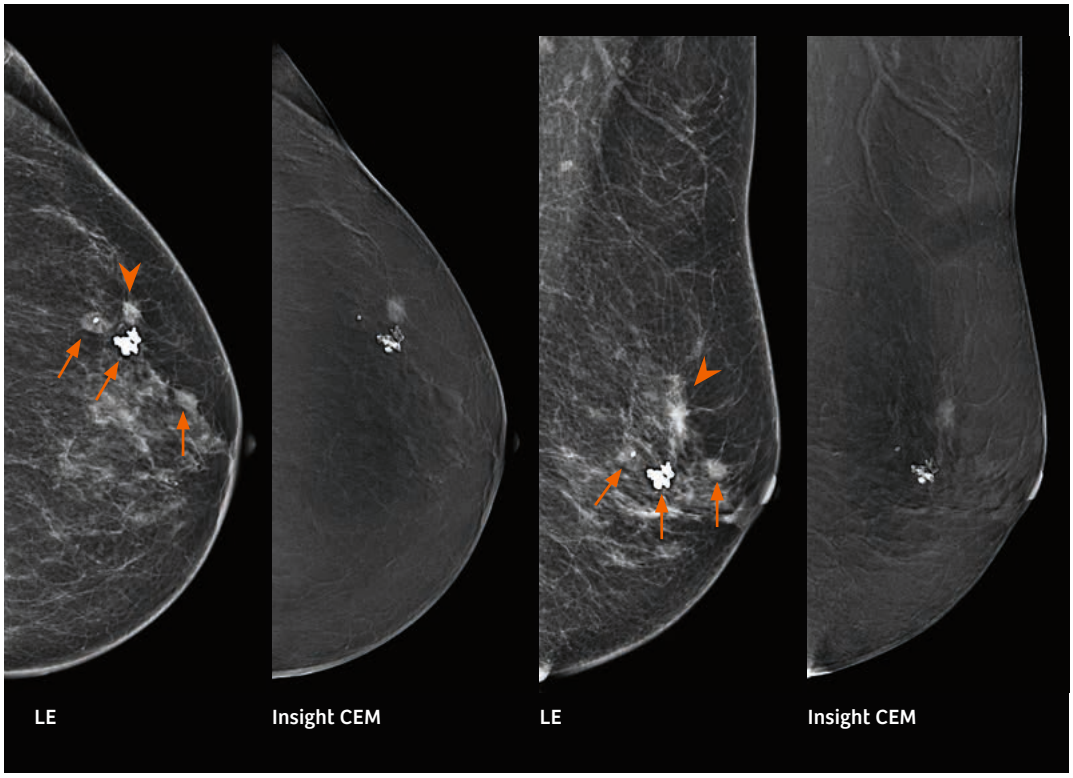

Figure 10: Clinical example of a 71-year-old asymptomatic female who underwent a TiCEM examination. The LE images of the left breast show one suspicious mass (arrow head) and three fibroadenomas (arrows), one of them being calcified. On the Insight CEM images the three fibroadenomas did not enhance, as expected (see 5.1). The suspicious mass showed contrast agent uptake and was proven to be a 4-mm IDC with associated DCIS. (Images courtesy of Dr. L. Pina, Pamplona, Spain)

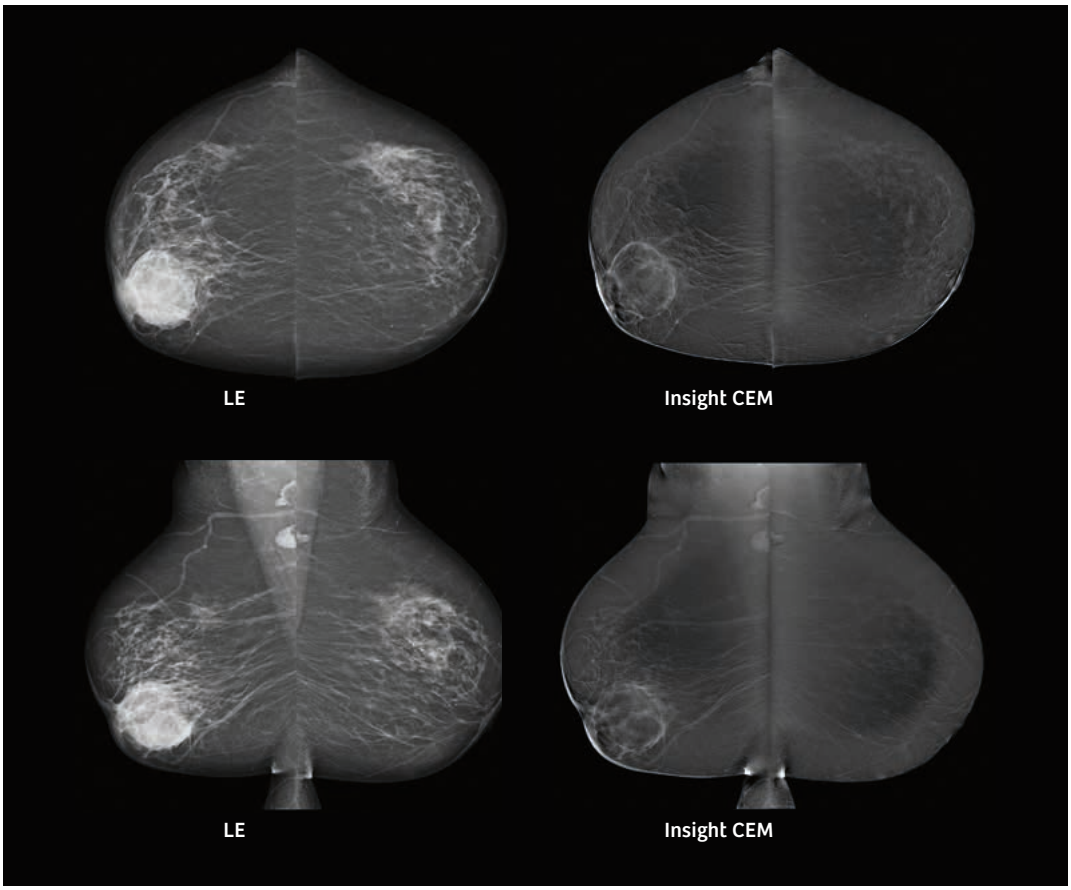

Figure 11: Clinical example of a 56-year-old woman presenting redness and warming of the skin. The LE images of the right breast show a retromammilar unsharp 37-mm lesion suspicious for abscess. The Insight CEM images do not show contrast agent uptake inside the lesion, whereas the boundary area shows enhancement, being indicative for a chronic active inflammation. Histology confirmed this lesion to be an abscess (benign finding). (Images courtesy of Prof. Dr. D. Uhlenbrock, Dortmund, Germany)

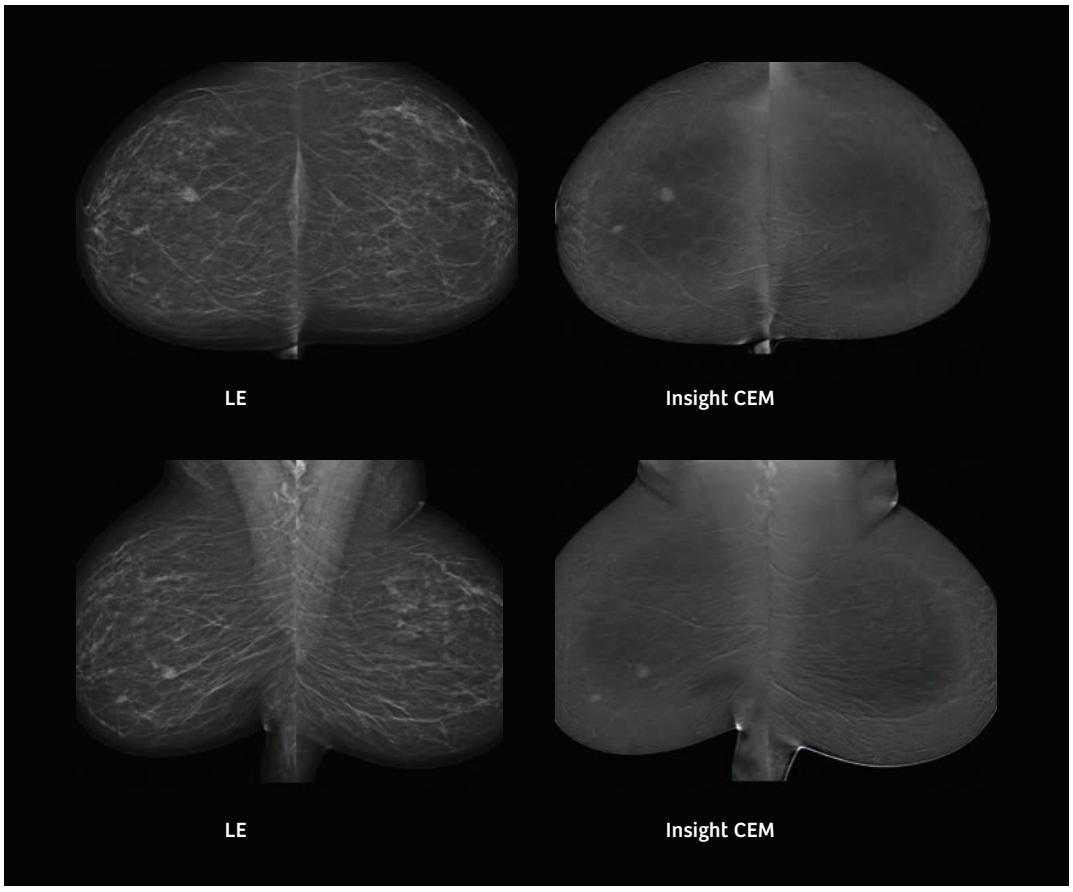

Figure 12: Clinical example of a 60-year-old woman who underwent a TiCEM examination. The LE images of the left breast show two suspicious lesions inside the fatty breast. The Insight CEM images show contrast agent uptake inside these lesions, being indicative for malignancy, which was confirmed by histology (IDC). (Images courtesy of Dr. I. Vejborg, Copenhagen, Denmark)

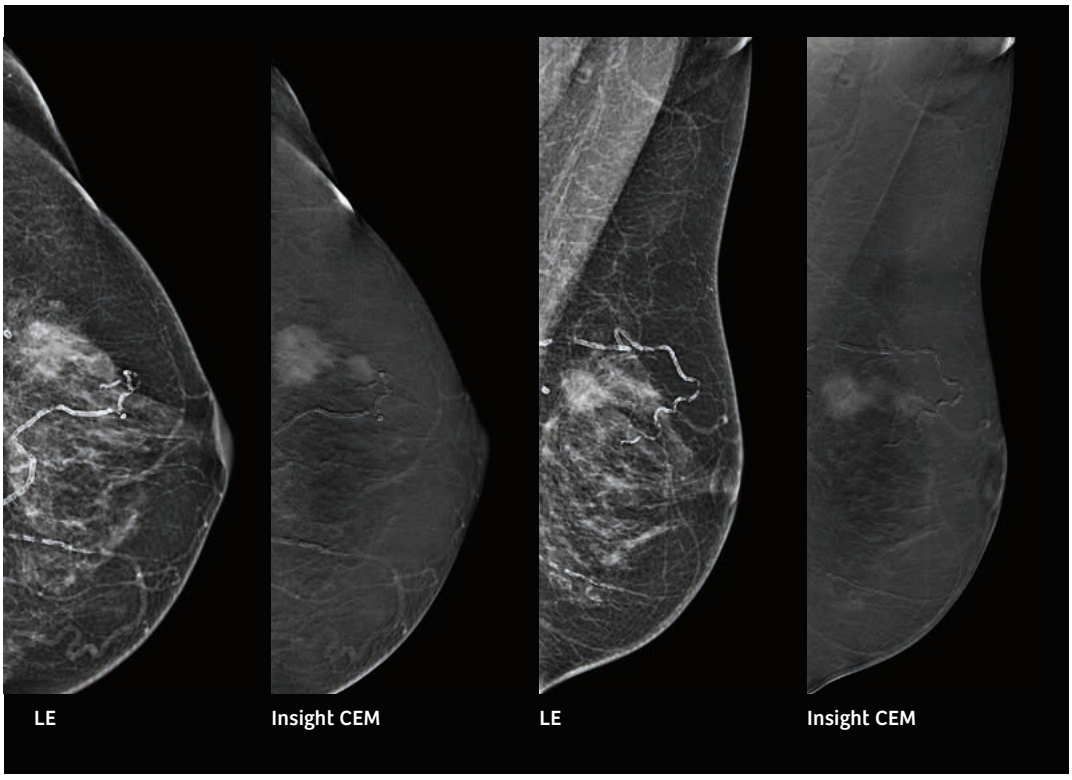

Figure 13: Clinical example of a 71-year-old female with a palpable lump in her left breast who underwent a TiCEM examination. The LE images show an irregular mass, but as the margins are not clearly seen, it is difficult to assess the cancer size. The Insight CEM images clearly show the size and extent of the lesion, which was proven to be a 30-mm invasive lobular carcinoma. (Images courtesy of Dr. L. Pina, Pamplona, Spain)

6. Discussion & conclusions

Currently, neither European nor American guidelines for contrast-enhanced dual-energy mammography exist. Consequently, there are no recommended acquisition and injection protocols, and image interpretation is reader-dependent. Further investigations are needed to find out the indications for which TiCEM is the method of choice compared to the other imaging modalities that are available for women requiring diagnostic workup. These future studies should be performed in unselected cases, since the currently available evidence is highly biased due to the fact that it is based on study cohorts with extremely high proportions of breast cancer [47].

6.1 Clinical indications for TiCEM

Since the physiological processes imaged with TiCEM are similar to breast MRI, it is expected that many indications for breast MRI could also apply to TiCEM. The most probable indications would then be:

- Clarification of inconclusive findings after conventional imaging or ultrasound
- Detection of occult lesions
- Pre-operative staging, assessment of multifocality and multicentricity
- Monitoring of the effectiveness of neo-adjuvant systemic therapy

Because of the contrast agent injection, TiCEM will most probably only be used for diagnostic workup, and not considered for breast screening.

6.2 Comparison with MRI

To date, breast MRI is the gold standard functional imaging technique for women requiring diagnostic workup. Guidelines for image acquisition and image interpretation exist [48] and clinical indications have been defined. However, MRI also has some disadvantages compared to TiCEM, potentially making the latter a cost-effective alternative to MRI (see Table 3).

Advantages of breast MRI and TiCEM	**Breast MRI**	**TiCEM**
Standard of care in diagnostic workup	●	
Imaging both breasts simultaneously	●	
No radiation dose	●	
No breast compression necessary	●	
Dynamic imaging possible	●	
Better availability		●
Lower costs		●
Shorter examination time		●
Improved workflow		●
Imaging of calcifications		●
Imaging of patients with implants / pacemaker		●
Imaging of patients with claustrophobia		●
Imaging possible for patients unable to assume prone position		●

Table 3: Advantages of breast MRI and TiCEM

Direct comparison of contrast-enhanced MRI examinations with TiCEM images should be made with caution. Although contrast agent behavior is expected to be the same [30] and some studies found good correlation between the two techniques [11, 13], the image contrasts are based on different physical principles: X-ray attenuation (TiCEM) versus magnetic susceptibility (MRI). In the case of MRI, a very high sensitivity and thus high signal for the gadolinium-based contrast agent can be achieved by selecting the right imaging sequence, even at very low concentrations of the contrast agent. X-ray attenuation, by contrast, is not sensitive to the iodinated contrast agent alone and follows the regular laws governing X-ray absorption, which is dependent on the materials imaged, their thicknesses and densities, and on the X-ray energies.

The scientific literature delivers mixed results in studies comparing the diagnostic performance of breast MRI with CEDEM. Some studies conclude in favor of CEDEM, with e.g. a lower number of false positive findings [16, 28, 33] and lower number of false negative findings for CEDEM compared to MRI [32]. At the same time, other studies report a higher false negative rate for CEDEM [42] and a lower cancer detection rate of index cancers for CEDEM compared to breast MRI [42, 33]. The results of these studies should, however, be interpreted with caution, as the study setups differed, the case numbers were very low and the inclusion criteria, imaging equipment, injection protocols and image interpretations differed between the studies.

One scientific study from Patel et al concludes that CEDEM is a cost-effective modality and a realistic substitute for breast MRI [49]. However, that publication uses sensitivity and specificity values that come from studies suffering from selection bias (see paragraph 5.1) and will most probably give too optimistic a picture of CEDEM. Whether CEDEM will become a cost-effective alternative to breast MRI is currently unknown and will depend on the scientific and technological developments that will take place in both modalities over the coming years.

6.3 Combinations with other technologies

In principle, the TiCEM approach could be combined with other technologies such as tomosynthesis, grid-less acquisition (PRIME) and biopsy.

The use of contrast-enhanced dual-energy tomosynthesis (CEDET) is still in an early experimental phase, and only a few groups have been conducting research on this subject [50–55]. Most notably, the group under W. Zhao [54] is investigating the potential role of CEDET with a Siemens Healthineers prototype system studying acquisition physics and protocols. Of particular interest is the lesion localization capability in 3D with CEDET. However, in the scientific literature, there is no consensus on whether this combination might deliver valuable additional diagnostic information, as compared with that provided by TiCEM and tomosynthesis as standalone techniques [56].

Siemens Healthineers' PRIME technology, enabling dose reduction through grid-less acquisition, might help to reduce the radiation dose in TiCEM examinations significantly. However, because of the different X-ray scatter properties with LE and HE spectra, as well as the complexity of the image recombination process, application of PRIME to TiCEM examinations is challenging and currently under evaluation in a clinical study.

Based on the rationale of performing an image-guided biopsy with the same modality that was used to detect the lesion, CEDEM-guided biopsy might become a clinical need in the future and has already been discussed in the scientific community [57, 58].

6.4 Conclusions

Siemens Healthineers launched TiCEM with its unique HE spectrum and an optimized titanium filter, which reduces X-ray tube load to enable seamless examinations. TiCEM delivers additional diagnostic information for more confident decision-making and helps to detect or rule out lesions. Being an integrated functionality of the MAMMOMAT Revelation, TiCEM can help reduce scheduling conflicts and workload on other modalities and could become a cost-effective alternative to breast MRI. Finally, guidelines are needed to achieve international standards in acquisition techniques and image interpretation.

7. Abbreviations

2D / 3D	two-dimensional / three-dimensional
AGD	average glandular dose
BPE	background parenchymal enhancement
CE	contrast-enhanced
CEDEM	contrast-enhanced dual-energy mammography
CEDET	contrast-enhanced dual-energy tomosynthesis
CT	computed tomography
DBT	digital breast tomosynthesis
DCE	dynamic contrast-enhanced
DCIS	ductal carcinoma in situ
DE	dual-energy
DXA	dual-energy X-ray absorptiometry
FFDM	full-field digital mammography
HE	high-energy
ICRU	International Commission on Radiation Units & Measurements
IDC	invasive ductal carcinoma
Insight CEM	recombined image from TiCEM
LE	low-energy
MRI	magnetic resonance imaging
***syngo*.Breast Care**	mammography reading solution for advanced visualization
TiCEM	titanium contrast-enhanced mammography
US	ultrasound

8. References

1. Perry N, Broeders MJM, de Wolf C, Törnberg S, Holland R, von Karsa L (2008) European guidelines for quality assurance in breast cancer screening and diagnosis. Fourth edition — summary document. Annals of oncology, official journal of the European Society for Medical Oncology / ESMO 19(4):614–22.

2. Skaane P, Bandos AI, Gullien R, Eben EB, Ekseth U, Haakenaasen U et al. (2013) Comparison of digital mammography alone and digital mammography plus tomosynthesis in a population-based screening program. Radiology 267(1):47–56.

3. Friedewald SM, Rafferty EA, Rose SL, Durand MA, Plecha DM, Greenberg JS et al. (2014) Breast cancer screening using tomosynthesis in combination with digital mammography. JAMA 311(24):2499–507.

4. Lång K, Andersson I, Rosso A, Tingberg A, Timberg P, Zackrisson S (2016) Performance of one-view breast tomosynthesis as a stand-alone breast cancer screening modality: results from the Malmo Breast Tomosynthesis Screening Trial, a population-based study. European radiology 26(1):184–90.

5. Bae KT (2010) Intravenous contrast medium administration and scan timing at CT: considerations and approaches. Radiology 256(1):32–61.

6. Strijkers GJ, Mulder WJM, van Tilborg GAF, Nicolay K (2007) MRI contrast agents: current status and future perspectives. Anti-cancer agents in medicinal chemistry 7(3):291–305.

7. Calliada F, Campani R, Bottinelli O, Bozzini A, Sommaruga MG (1998) Ultrasound contrast agents: basic principles. European journal of radiology 27 Suppl 2:S157-60.

8. Tofts PS, Brix G, Buckley DL, Evelhoch JL, Henderson E, Knopp MV et al. (1999) Estimating kinetic parameters from dynamic contrast-enhanced T(1)-weighted MRI of a diffusable tracer: standardized quantities and symbols. Journal of magnetic resonance imaging JMRI 10(3):223–32.

9. Parker GJM, Buckley DL (2005) Tracer Kinetic Modelling for T1-Weighted DCE-MRI. In: Jackson A, Buckley DL, Parker GJM (eds) Dynamic Contrast-Enhanced Magnetic Resonance Imaging in Oncology. Springer-Verlag Berlin Heidelberg. Berlin Heidelberg, pp 81–92.

10. Ah-See M-LW, Padhani AR (2005) Dynamic Magnetic Resonance Imaging in Breast Cancer. In: Jackson A, Buckley DL, Parker GJM (eds) Dynamic Contrast-Enhanced Magnetic Resonance Imaging in Oncology. Springer-Verlag Berlin Heidelberg. Berlin Heidelberg, pp 145–173.

11. Sogani J, Morris EA, Kaplan JB, D'Alessio D, Goldman D, Moskowitz CS et al. (2017) Comparison of Background Parenchymal Enhancement at Contrast-enhanced Spectral Mammography and Breast MR Imaging. Radiology 282(1): 63-73.

12. Lewis TC, Patel BK, Pizzitola VJ (2017) Navigating contrast-enhanced digital mammography. Appl radiol 46(3):21–8.

13. Knogler T, Homolka P, Hoernig M, Leithner R, Langs G, Waitzbauer M et al. (2017) Application of BI-RADS Descriptors in Contrast-Enhanced Dual-Energy Mammography: Comparison with MRI. Breast care (Basel, Switzerland) 12(4):212–6.

14. Savaridas SL, Taylor DB, Gunawardana D, Phillips M (2017) Could parenchymal enhancement on contrast-enhanced spectral mammography (CESM) represent a new breast cancer risk factor? Correlation with known radiology risk factors. Clinical radiology 72(12):1085.e1-1085.e9.

15. Carmeliet P, Jain RK (2000) Angiogenesis in cancer and other diseases. Nature 407(6801):249–57.

16. Lobbes MBI, Smidt ML, Houwers J, Tjan-Heijnen VC, Wildberger JE (2013) Contrast enhanced mammography: techniques, current results, and potential indications. Clinical radiology 68(9):935–44.

17. Jong RA, Yaffe MJ, Skarpathiotakis M, Shumak RS, Danjoux NM, Gunesekara A et al. (2003) Contrast-enhanced digital mammography: initial clinical experience. Radiology 228(3):842–50.

18. Lehman CD, Gatsonis C, Kuhl CK, Hendrick E, Pisano ED, Hanna L et al. (2007) MRI evaluation of the contralateral breast in women with recently diagnosed breast cancer. The New England journal of medicine 356(13):1295–303.

19. Mann RM, Kuhl CK, Kinkel K, Boetes C (2008) Breast MRI: guidelines from the European Society of Breast Imaging. European radiology 18(7):1307–18.

20. Diekmann F, Diekmann S, Jeunehomme F, Muller S, Hamm B, Bick U (2005) Digital mammography using iodine-based contrast media: initial clinical experience with dynamic contrast medium enhancement. Investigative radiology 40(7):397–404.

21. Lalji UC, Jeukens CRLPN, Houben I, Nelemans PJ, van Engen RE, van Wylick E et al. (2015) Evaluation of low-energy contrast-enhanced spectral mammography images by comparing them to full-field digital mammography using EUREF image quality criteria. European radiology 25(10):2813–20.

22. Thomsen HS, Webb JAW (eds.) (2014) Contrast media: Safety issues and ESUR guidelines, 3rd ed. Springer, Heidelberg, New York, NY, Dordrecht, London, Berlin.

23. American College of Radiology (2015) ACR manual on contrast media, 10th ed. American College of Radiology, Reston, VA.

24. Hubbell JH, Seltzer SM (1996) Tables of X-Ray Mass Attenuation Coefficients and Mass Energy-Absorption Coefficients from 1 keV to 20 MeV for Elements Z = 1 to 92 and 48 Additional Substances of Dosimetric Interest: NISTIR 5632; Available via http://www.nist.gov/pml/data/xraycoef/.

25. Dromain C, Thibault F, Diekmann F, Fallenberg EM, Jong RA, Koomen M et al. (2012) Dual-energy contrast-enhanced digital mammography: initial clinical results of a multireader, multicase study. Breast cancer research BCR 14(3):R94.

26. Lalji UC, Houben IPL, Prevos R, Gommers S, van Goethem M, Vanwetswinkel S et al. (2016) Contrast-enhanced spectral mammography in recalls from the Dutch breast cancer screening program: validation of results in a large multireader, multicase study. European radiology 26(12):4371–9.

27. Houben IPL, van de Voorde P, Jeukens, C R L P N, Wildberger JE, Kooreman LF, Smidt ML et al. (2017) Contrast-enhanced spectral mammography as work-up tool in patients recalled from breast cancer screening has low risks and might hold clinical benefits. European journal of radiology 94:31–7.

28. Jochelson MS, Dershaw DD, Sung JS, Heerdt AS, Thornton C, Moskowitz CS et al. (2013) Bilateral contrast-enhanced dual-energy digital mammography: feasibility and comparison with conventional digital mammography and MR imaging in women with known breast carcinoma. Radiology 266(3):743–51.

29. Cheung Y-C, Juan Y-H, Lin Y-C, Lo Y-F, Tsai H-P, Ueng S-H et al. (2016) Dual-Energy Contrast-Enhanced Spectral Mammography: Enhancement Analysis on BI-RADS 4 Non-Mass Microcalcifications in Screened Women. PloS one 11(9):e0162740.

30. Lewis TC, Pizzitola VJ, Giurescu ME, Eversman WG, Lorans R, Robinson KA et al. (2017) Contrast-enhanced Digital Mammography: A Single-Institution Experience of the First 208 Cases. The breast journal 23(1):67–76.

31. Patel BK, Garza SA, Eversman S, Lopez-Alvarez Y, Kosiorek H, Pockaj BA (2017) Assessing tumor extent on contrast-enhanced spectral mammography versus full-field digital mammography and ultrasound. Clinical imaging 46:78–84.

32. Wang Q, Li K, Wang L, Zhang J, Zhou Z, Feng Y (2016) Preclinical study of diagnostic performances of contrast-enhanced spectral mammography versus MRI for breast diseases in China. SpringerPlus 5(1):763.

33. Lee-Felker SA, Tekchandani L, Thomas M, Gupta E, Andrews-Tang D, Roth A et al. (2017) Newly Diagnosed Breast Cancer: Comparison of Contrast-enhanced Spectral Mammography and Breast MR Imaging in the Evaluation of Extent of Disease. Radiology 285(2):389–400.

34. Yagil Y, Shalmon A, Rundstein A, Servadio Y, Halshtok O, Gotlieb M et al. (2016) Challenges in contrast-enhanced spectral mammography interpretation: artefacts lexicon. Clinical radiology 71(5):450–7.

35. Łuczyńska E, Heinze-Paluchowska S, Hendrick E, Dyczek S, Ryś J, Herman K et al. (2015) Comparison between breast MRI and contrast-enhanced spectral mammography. Medical science monitor: international medical journal of experimental and clinical research 21:1358–67.

36. Knogler T, Homolka P, Hörnig M, Leithner R, Langs G, Waitzbauer M et al. (2015) Contrast-enhanced dual energy mammography with a novel anode / filter combination and artifact reduction: a feasibility study. European radiology. doi:10.1007/s00330-015-4007-6.

37. Gluskin J, Click M, Fleischman R, Dromain C, Morris EA, Jochelson MS (2017) Contamination artifact that mimics in-situ carcinoma on contrast-enhanced digital mammography. European journal of radiology 95:147–54.

38. Bhimani C, Li L, Liao L, Roth RG, Tinney E, Germaine P (2017) Contrast-enhanced Spectral Mammography: Modality-Specific Artifacts and Other Factors Which May Interfere with Image Quality. Academic radiology 24(1):89–94.

39. Hörnig M, Bätz L, Mertelmeier T (2012) Design of a contrast-enhanced dual-energy tomosynthesis system for breast cancer imaging. In: Pelc NJ, Nishikawa RM, Whiting BR (eds) Medical imaging 2012: physics of medical imaging: 5-8 February 2012, San Diego, California, United States. SPIE. Bellingham, Wash., 83134O.

40. Mohamed Kamal R, Hussien Helal M, Wessam R, Mahmoud Mansour S, Godda I, Alieldin N (2015) Contrast-enhanced spectral mammography: Impact of the qualitative morphology descriptors on the diagnosis of breast lesions. European journal of radiology 84(6):1049–55.

41. Daniaux M, Santner W, de Zordo T(2015) A new tool in mammography: contrast-enhanced dual energy mammography. Di Europe, Sept. 2015.

42. Thibault F, Balleyguier C, Tardivon A, Dromain C (2012) Contrast enhanced spectral mammography: Better than MRI? European journal of radiology 81:S162-S164.

43. Tennant SL, James JJ, Cornford EJ, Chen Y, Burrell HC, Hamilton LJ et al. (2016) Contrast-enhanced spectral mammography improves diagnostic accuracy in the symptomatic setting. Clinical radiology 71(11):1148–55.

44. Watanabe M (2014) The effectiveness of dual-energy contrast-enhanced digital mammography for Japanese Women – The pathological considerations. European Congress of Radiology.

45. Patel BK, Ranjbar S, Wu T, Pockaj BA, Li J, Zhang N et al. (2018) Computer-aided diagnosis of contrast-enhanced spectral mammography: A feasibility study. European journal of radiology 98:207–13.

46. Patel BK, Naylor ME, Kosiorek HE, Lopez-Alvarez YM, Miller AM, Pizzitola VJ et al. (2017) Clinical utility of contrast-enhanced spectral mammography as an adjunct for tomosynthesis-detected architectural distortion. Clinical imaging 46:44–52.

47. Tagliafico A, Rossi F, Signori A, Sormani MP, Valdora F, Calabrese M et al. (2016) Diagnostic performance of contrast-enhanced spectral mammography: Systematic review and meta-analysis. Breast (Edinburgh, Scotland) 28:13–9.

48. D'Orsi CJ (ed.) (2014) ACR BI-RADS® Atlas: Breast Imaging Reporting and Data System 2013. Mammography, Ultrasound, Magnetic Resonance Imaging, Follow-up and Outcome Monitoring, Data Dictionary, 5th ed. American College of Radiology, Reston VA.

49. Patel BK, Gray RJ, Pockaj BA (2017) Potential Cost Savings of Contrast-Enhanced Digital Mammography. AJR. American journal of roentgenology 208(6):W231-W237.

50. Carton A-K, Gavenonis SC, Currivan JA, Conant EF, Schnall MD, Maidment ADA (2010) Dual-energy contrast-enhanced digital breast tomosynthesis – a feasibility study. The British journal of radiology 83(988):344–50.

51. Hu Y-H, Zhao W (2011) A 3D linear system model for the optimization of dual-energy contrast-enhanced digital breast tomosynthesis. In: Pelc NJ (ed) Medical imaging 2011: physics of medical imaging: 13 - 17 February 2011, Lake Buena Vista, Florida, United States. SPIE. Bellingham, Wash., 79611C-79611C-9.

52. Schmitzberger FF, Fallenberg EM, Lawaczeck R, Hemmendorff M, Moa E, Danielsson M et al. (2011) Development of low-dose photon-counting contrast-enhanced tomosynthesis with spectral imaging. Radiology 259(2):558–64.

53. Froeling V, Diekmann F, Renz DM, Fallenberg EM, Steffen IG, Diekmann S et al. (2013) Correlation of contrast agent kinetics between iodinated contrast-enhanced spectral tomosynthesis and gadolinium-enhanced MRI of breast lesions. European radiology 23(6):1528–36.

54. Hu Y-H, Scaduto DA, Zhao W (2013) Optimization of clinical protocols for contrast enhanced breast imaging. In: Nishikawa RM, Whiting BR, Hoeschen C (eds) Medical imaging 2013: 11-14 February 2013, Lake Buena Vista, Florida, United States. SPIE. Bellingham, Washington, 86680G-86680G-9.

55. Chou C-P, Lewin JM, Chiang C-L, Hung B-H, Yang T-L, Huang J-S et al. (2015) Clinical evaluation of contrast-enhanced digital mammography and contrast enhanced tomosynthesis – Comparison to contrast-enhanced breast MRI. European journal of radiology 84(12):2501–8.

56. Lobbes MBI, Houben I (2016) Contrast-enhanced tomosynthesis: The best of both worlds or more of the same? European journal of radiology 85(2):507–8.

57. Dromain C, Canale S, Saab-Puong S, Carton A-K, Muller S, Fallenberg EM (2014) Optimization of contrast-enhanced spectral mammography depending on clinical indication. Journal of medical imaging (Bellingham, Wash.) 1(3):33506.

58. Luczyńska E, Heinze S, Adamczyk A, Rys J, Mitus JW, Hendrick E (2016) Comparison of the Mammography, Contrast-Enhanced Spectral Mammography and Ultrasonography in a Group of 116 patients. Anticancer research 36(8):4359–66.

On account of certain regional limitations of sales rights and service availability, we cannot guarantee that all products / services / features included in this brochure are available through the Siemens Healthineers sales organization worldwide. Availability and packaging may vary by country and are subject to change without prior notice.

The information in this document contains general descriptions of the technical options available and may not always apply in individual cases.

Siemens Healthineers reserves the right to modify the design and specifications contained herein without prior notice. Please contact your local Siemens Healthineers sales representative for the most current information.

In the interest of complying with legal requirements concerning the environmental compatibility of our products (protection of natural resources and waste conservation), we may recycle certain components where legally permissible. For recycled components we use the same extensive quality assurance measures as for factory-new components.

Any technical data contained in this document may vary within defined tolerances. Original images always lose a certain amount of detail when reproduced.

Siemens Healthineers Headquarters
Siemens Healthcare GmbH
Henkestr. 127
91052 Erlangen, Germany
Phone: +49 9131 84-0
siemens-healthineers.com

Published by Siemens Healthcare GmbH · PDF only · 6323 0718 · ©Siemens Healthcare GmbH, 2018